

## CHAPTER III

### A GENERAL APPROACH TO SINE COMPARATORS

#### 3.1 INTRODUCTION :

A static distance relay working on the principle of phase comparison of the system quantities makes use of either block-block scheme or block-spike scheme. The former scheme compares the system quantities directly in a phase comparator followed by an integrator and a level detector. Comparator models described by Humpage and Sabberwal<sup>20</sup> and Giot, Marchal and Vasquez<sup>19</sup>, working on this principle, give improved polar characteristics that invoke the use of reduced angular limits of phase comparison. But these arrangements necessitate time delay to complete phase comparison in addition to certain logic operations. Further, the necessity of employing  $n(n-1)/2$  signals for obtaining  $n$  line segments of the pick-up characteristic, employing symmetrical comparison limits, results in a complicated measuring circuit of the relay and an inferior control of the line segments. In many cases it becomes difficult to avoid the unwanted line segments appearing in the composite tripping characteristic.

On the other hand, in block-spike scheme a spike is produced at the zero cross-over of the operating signal and is compared with polarising signals for the phase. The

static mho distance relay described by Dewey, Mathews and Morris employs this scheme which provides the fastest measurement of the direction<sup>30</sup>. The security and reliability of this scheme have been amply verified by staged fault tests and by a period of field experience<sup>31</sup>.

Parthasarathy developed a multi-input phase comparator model employing symmetrical comparison limits, which yielded quadrilateral pick-up characteristic<sup>32</sup>. Subsequently, Anilkumar and Parthasarathy reported the mathematical basis of sine comparators ( block-spike scheme ) taking into account only the symmetrical comparison limits<sup>33</sup>.

The purpose of the present chapter is, to develop the mathematical basis of sine comparators so as to foot the comparator on completely general basis and to report a relaying scheme employing unsymmetrical limits of phase comparison.

### 3.2 ANALYSIS OF DISTANCE RELAYS :

The distance relays are usually analysed on R-X diagram of the protected transmission line. Fig.3.1 shows a typical power system and fig.3.2 shows the R-X diagram of the protected transmission line under consideration.

In fig.3.2 LM represents the power swing locus. This locus will be a straight line for equal voltages at the two



ends of the protected transmission line, and it will be an arc of a circle for unequal voltages. However, for all practical purposes of distance relay analysis it may be assumed to be a straight line.

The relay characteristic to be employed for the transmission line protection should snugly fit around the fault area so as to be least vulnerable to power swings and faults on the other phase or phases.

### 3.3 MATHEMATICAL BASIS OF 2-INPUT SINE COMPARATORS :

#### 3.3.1 Basic Equations :

Let the inputs to the sine comparator be of the form :

$$\begin{aligned} S_1 &= K_1 \angle \alpha_1 V_L \angle 0 + Z_{R_1} I_L \angle \theta_1 - \phi & \begin{matrix} 0 \\ 0 \\ 0 \\ 0 \\ 0 \end{matrix} \\ \text{and } S_2 &= K_2 \angle \alpha_2 V_L \angle 0 + Z_{R_2} I_L \angle \theta_2 - \phi & \dots (3.1) \end{aligned}$$

Where  $V_L$  and  $I_L$  are the fault voltage and current referred to the secondaries of potential and current transformers respectively, and  $\phi$  is the angle between  $V_L$  and  $I_L$ . Constants  $K_1 \angle \alpha_1$  and  $K_2 \angle \alpha_2$  are the complex coefficients of  $V_L$ . In most of the cases they are real numbers less than or equal to one. However they are treated here as complex to make the analysis completely general. The replica impedances  $Z_{R_1} \angle \theta_1$  and  $Z_{R_2} \angle \theta_2$  are introduced into the measuring circuits, which usually help in improving

the transient performance of the relay<sup>46</sup>.

On expressing the signals in the form

$$S_1 = a + jb$$

and  $S_2 = c + jd$

it can be shown<sup>33</sup> that the condition for the tripping pulse to emerge is

$$\frac{bc - ad}{\sqrt{(a^2 + b^2)(c^2 + d^2)}} \leq \sin \beta \quad \dots (3.2)$$

Where  $\beta = \beta_1$  and  $\beta_2$  are the limits of comparison.

Fig.3.3 shows the block-schematic diagram of a 2-input comparator and fig.3.4 shows the mode of comparison. System quantities  $V_L$  and  $I_L$  are applied to the measuring circuit (M) which produces the required signals  $S_1$  and  $S_2$ .  $P_1$  and  $P_2$  produce the necessary pulses from  $S_1$  and  $S_2$  at their zero cross-overs. Pulse from  $S_2$  is used to obtain the desired unsymmetry in phase comparison and then compared with the pulse from  $S_1$ . The AND gate provides output pulse only if at the time of the arrival of the pulse from  $S_1$  in the gate, the modified polarising signal  $S_2$  is -ve .

Inequality(3.2) can be written as

$$bc - ad \leq \pm \tan \beta (ac + bd) \quad \dots (3.3)$$

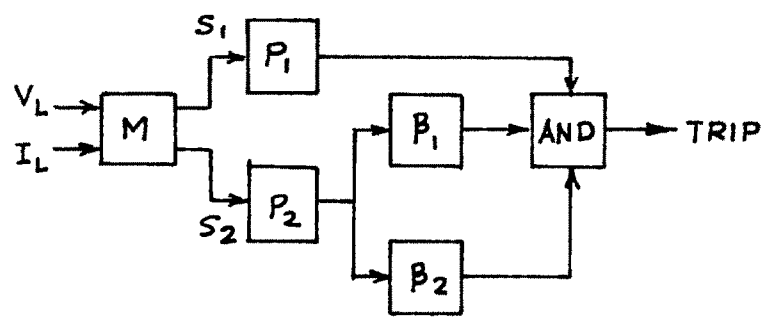


FIG. 3-3 BLOCK-SCHEMATIC DIAGRAM OF THE RELAY

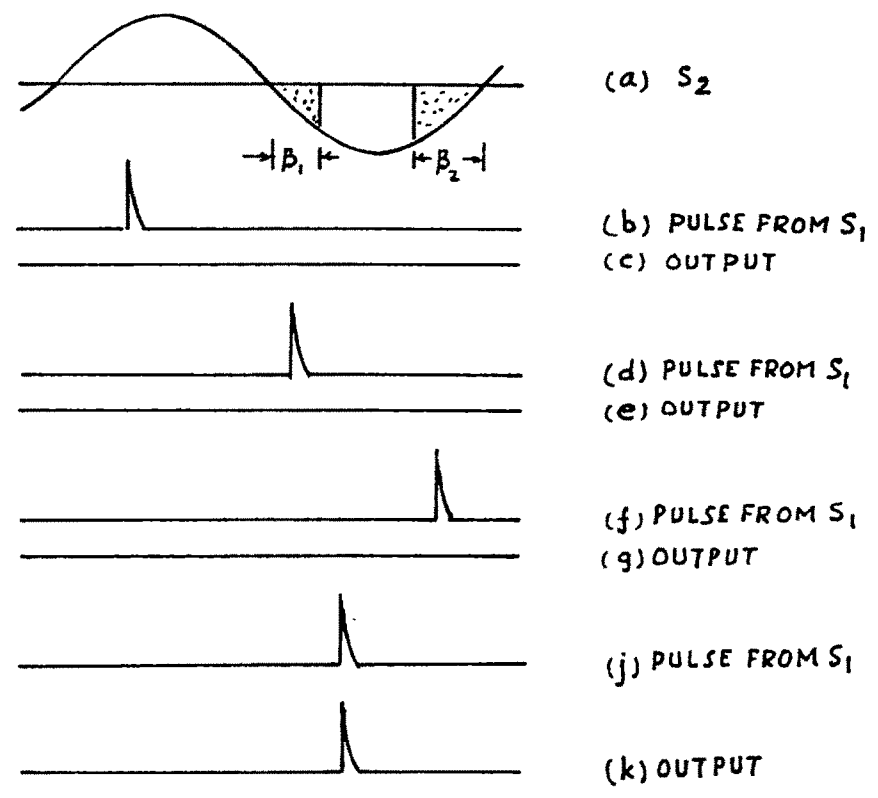


FIG. 3-4 MODE OF COMPARISON

where

$$\begin{aligned}
 a &= K_1 V_L \cos \alpha_1 + Z_{R_1} I_L \cos (\theta_1 - \phi) \\
 b &= K_1 V_L \sin \alpha_1 + Z_{R_1} I_L \sin (\theta_1 - \phi) \\
 c &= K_2 V_L \cos \alpha_2 + Z_{R_2} I_L \cos (\theta_2 - \phi) \\
 d &= K_2 V_L \sin \alpha_2 + Z_{R_2} I_L \sin (\theta_2 - \phi)
 \end{aligned}
 \tag{3.4}$$

For the symmetrical comparison limits of  $\pi$  and  $2\pi$ , both  $\beta_1$  and  $\beta_2$  will be zero. Substituting (3.4) into (3.3) and letting  $\beta_1 = \beta_2 = 0$  inequality (3.3) will reduce to

$$\begin{aligned}
 &K_1 K_2 (R^2 + X^2) \sin(\alpha_1 - \alpha_2) + R [ K_1 Z_{R_2} \sin(\alpha_1 - \theta_2) \\
 &+ K_2 Z_{R_1} \sin(\theta_1 - \alpha_2) ] + X [ K_1 Z_{R_2} \cos(\alpha_1 - \theta_2) \\
 &- K_2 Z_{R_1} \cos(\theta_1 - \alpha_2) ] + Z_{R_1} Z_{R_2} \sin(\theta_1 - \theta_2) \leq 0 \quad \dots(3.5)
 \end{aligned}$$

$$\begin{aligned}
 \text{Where, } R &= (V_L / I_L) \cos \phi \\
 \text{and } X &= (V_L / I_L) \sin \phi
 \end{aligned}
 \tag{3.6}$$

Inequality (3.5) represents a circle on R-X plane with tripping inside the circle if  $\alpha_1 > \alpha_2$  and outside the circle if  $\alpha_1 < \alpha_2$ .

In the general case of unsymmetrical limits of comparison inequality (3.3) can be written as

$$\begin{aligned}
& K_1 K_2 (R^2 + X^2) [ \sin(\alpha_1 - \alpha_2) - \tan \phi_1 \cos(\alpha_1 - \alpha_2) ] \\
& + R [ K_1 Z_{R_2} \sin(\alpha_1 - \theta_2) + K_2 Z_{R_1} \sin(\theta_1 - \alpha_2) \\
& - \tan \phi_1 \{ K_1 Z_{R_2} \cos(\alpha_1 - \theta_2) + K_2 Z_{R_1} \cos(\theta_1 - \alpha_2) \} ] \\
& + X [ K_1 Z_{R_2} \cos(\alpha_1 - \theta_2) - K_2 Z_{R_1} \cos(\theta_1 - \alpha_2) \\
& + \tan \phi_1 \{ K_1 Z_{R_2} \sin(\alpha_1 - \theta_2) - K_2 Z_{R_1} \sin(\theta_1 - \alpha_2) \} ] \\
& + Z_{R_1} Z_{R_2} [ \sin(\theta_1 - \theta_2) - \tan \phi_1 \cos(\theta_1 - \theta_2) ] \leq 0 \quad \dots(3.7)
\end{aligned}$$

and

$$\begin{aligned}
& K_1 K_2 (R^2 + X^2) [ \sin(\alpha_1 - \alpha_2) + \tan \phi_2 \cos(\alpha_1 - \alpha_2) ] \\
& + R [ K_1 Z_{R_2} \sin(\alpha_1 - \theta_2) + K_2 Z_{R_1} \sin(\theta_1 - \alpha_2) \\
& + \tan \phi_2 \{ K_1 Z_{R_2} \cos(\alpha_1 - \theta_2) + K_2 Z_{R_1} \cos(\theta_1 - \alpha_2) \} ] \\
& + X [ K_1 Z_{R_2} \cos(\alpha_1 - \theta_2) - K_2 Z_{R_1} \cos(\theta_1 - \alpha_2) \\
& - \tan \phi_2 \{ K_1 Z_{R_2} \sin(\alpha_1 - \theta_2) - K_2 Z_{R_1} \sin(\theta_1 - \alpha_2) \} ] \\
& + Z_{R_1} Z_{R_2} [ \sin(\theta_1 - \theta_2) + \tan \phi_2 \cos(\theta_1 - \theta_2) ] \leq 0 \quad \dots(3.8)
\end{aligned}$$

### 3.3.2 Graphical Construction For Circular Characteristics:

For the case of symmetrical limits of comparison of  $\pi$  and  $2\pi$  the necessary input signals can be chosen which satisfy inequality (3.5). However, it is laborious, and further, when the limits of comparison are completely

unsymmetrical, for which inequalities (3.7) and (3.8) must be satisfied simultaneously, the derivation of input signals becomes extremely complicated. Graphical construction is therefore developed and is shown in fig. 3.5. The construction is as follows: Two straight lines  $OA = Z_1$  and  $OB = Z_2$  are drawn at  $\angle \psi_1$  and  $\angle \psi_2$  respectively as shown. Line  $AB$ , then, is the common chord of the two circles represented by inequalities (3.7) and (3.8). Lines  $CA$  and  $CB$  are drawn each inclined at  $\angle \alpha_1 - \alpha_2 - 90^\circ$  to  $AB$ . The centres  $D$  and  $E$  of the two circles will lie on the line  $FG$  bisecting  $AB$  in  $H$ . Lines  $AE$  and  $AD$  are drawn at the respective angles  $\beta_1$  and  $\beta_2$  with respect to line  $AC$ . With centres  $D$  and  $E$ , two circles are drawn with the respective radii  $BD$  and  $BE$  representing the common region as the tripping region.

### 3.3.3 Rectilinear Characteristics- Basic Equations :

The mathematical basis developed in section 3.3.1 and the graphical construction for circular characteristics reported in section 3.3.2 will be useful in obtaining any circular characteristic. The particular characteristics of importance are mho and Offset mho. However, for the protection of long transmission lines, quadrilateral characteristic is more desirable which consists of four rectilinear segments. Mathematical basis of rectilinear characteristics are, therefore, developed in this section.



If in inequalities(3.7) and (3.8), following conditions are employed, the resulting inequalities will represent rectilinear characteristics:

$$\begin{aligned} K_1 &= -K_1 & \begin{matrix} 0 \\ 0 \\ 0 \\ 0 \end{matrix} & \dots(3.9) \\ K_2 &= 0 ; \alpha_2 = 0 & \begin{matrix} 0 \\ 0 \\ 0 \\ 0 \end{matrix} & \end{aligned}$$

On substituting the condition given by (3.9) in inequalities(3.7) and (3.8) the respective resulting inequalities would be :

$$X \leq -\tan(\alpha_1 - \theta_2 - \beta_1) R + \frac{Z_{R1}}{K_1} \left[ \frac{\sin(\theta_1 - \theta_2) - \tan\beta_1 \cos(\theta_1 - \theta_2)}{\cos(\alpha_1 - \theta_2) + \tan\beta_1 \sin(\alpha_1 - \theta_2)} \right]$$

....(3.10)

and,

$$X \leq -\tan(\alpha_1 - \theta_2 + \beta_2) R + \frac{Z_{R1}}{K_1} \left[ \frac{\sin(\theta_1 - \theta_2) + \tan\beta_2 \cos(\theta_1 - \theta_2)}{\cos(\alpha_1 - \theta_2) - \tan\beta_2 \sin(\alpha_1 - \theta_2)} \right]$$

....(3.11)

### 3.3.4 Graphical Construction :

The graphical construction corresponding to (3.10) and (3.11) is shown in fig.3.6. The construction is as follows: Line OK =  $Z_1$  is drawn at an angle  $\psi$  with respect to R-axis. From K line LM is drawn perpendicular to line OA drawn at  $\angle \delta$  with the R-axis. From K, KP and KQ inclined at the

respective angles  $\beta_1$  and  $\beta_2$  are drawn. The shaded region then is the tripping region.

### 3.4 A GENERAL ANALYSIS OF SINE COMPARATORS :

In section 3.3 the general mathematical basis are developed with reference to 2-input sine comparators. However they apply equally well to multi-input comparators. The voltage coefficients are treated as complex and unsymmetrical comparison limits are taken into account rendering the analysis completely general.

Depending upon the mode of comparison of the input signals, the sine comparators are classified into:

- (i) 2-input comparators, and
- (ii) Multi-input comparators.

#### 3.4.1 2-Input Comparators :

In a 2-input sine comparator, two complex signals  $S_1$  and  $S_2$  are derived from a measuring circuit. A positive going pulse is obtained from  $S_1$  (operating signal) at its zero cross-over when it changes its sign from negative to positive.  $S_1$  is then compared with  $S_2$  (polarising signal) for the phase. A typical phase comparator which could be employed for the purpose is shown in fig.3.7. It is evident that the output from the gate appears only if  $S_1$  leads  $S_2$ .

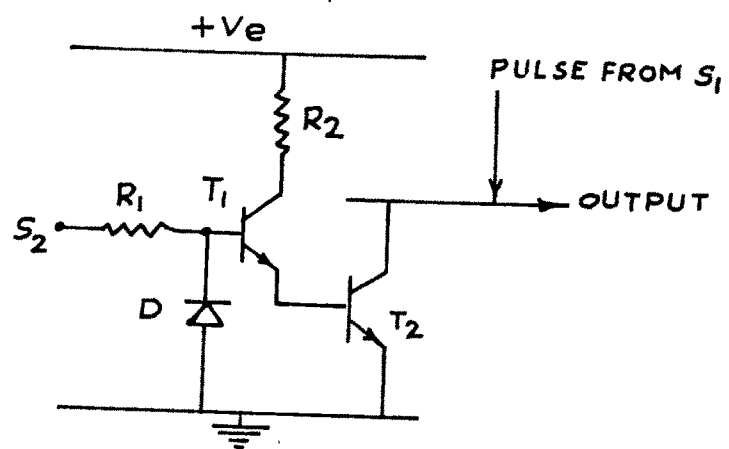


FIG. 3.7 2-INPUT COMPARATOR

When the required characteristic on the impedance plane has more than two discontinuities ( for example the quadrilateral characteristic of fig.3.8), the number of input signals to be compared will be more than two, resulting in more involved circuitry of the relay. Further, multi-winding, 1:1 transformers will be required for the purpose of isolation of the system quantities in the derivation of input signals rendering the transient performance of the relay inferior.

The large number of input signals and the requirement of the involved circuitry could be verified by considering the characteristic of fig.3.8. The necessary input signals for obtaining the line segment AB of the characteristic may be obtained as follows. If points  $P_1$  and  $P_2$  are selected as the tips of the vectors  $Z_{R_1} / K_1$  and  $Z_{R_2} / K_2$  ( as shown) and substituted in the analysis of section 3.3 a pair of required signals will be obtained. This pair of signals, in general, will be entirely different from the other pairs of signals obtained in similar manner for the remaining line segments. Each pair of signals when compared in an individual 2-input comparator will provide a line segment on the impedance plane. The pulse outputs of the individual comparators will be required to be stretched and AND compounded to superimpose the segments of the characteristic on the impedance plane.

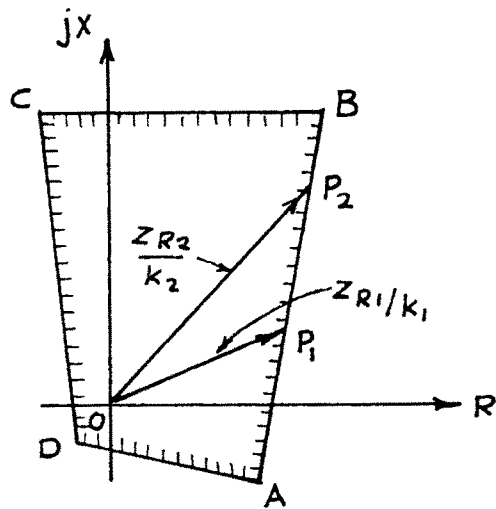


FIG. 3-8 QUADRILATERAL CHARACTERISTIC

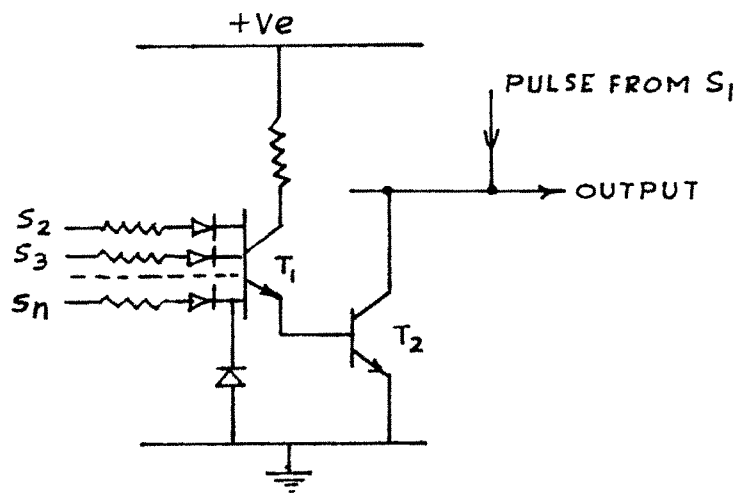


FIG. 3-9 MULTI-INPUT PHASE COMPARATOR

It is evident from the above that, in general  $2n$  number of input signals will be required to obtain a characteristic with  $n$  segments. For the purpose of phase comparison  $(n+1)$  comparators will be required,  $n$  being for the initial phase comparison (2-input type) and one final comparator (multi-input type) for AND compounding. Further  $(n-1)$  pulse stretching circuits will be required as the pulses cannot be compared directly in the final multi-input comparator due to their different times of occurrence.

Thus the relay employing this type of comparators will involve a large number of circuit components. A distinct advantage, however, of this type of relay is that each line segment of the final tripping characteristic is independently controllable. The advantage of the independent control of the segments of the characteristic may be appreciated from the following consideration.

The distance relays are generally used in a double role viz. (i) to provide primary protection to the section of the transmission line under consideration, and (ii) back-up protection to the section under consideration and the next or previous section. The back-up protection is usually in two steps with different time delays.

When a common phase comparator is to be employed for all the three steps of operation, the relay will be required to change its setting from zone-1 reach to zone-2 reach and from zone-2 reach to zone-3 reach. In this process the reach on both resistance and reactance axis are required to be changed. The resistance reach is required to be changed due to the fact that the fault arc resistance provided by the arc during lightning (the major cause of faults) is different in the three zones of protection. Since the first zone faults are to be cleared in about 2 or 3 cycles (40 to 60 msec.) the effect of cross-wind on the arc will be insignificant. However, 2nd and 3rd zone faults are to be cleared only after time delays, the larger resistance reach will be required due to the stretching of arcs caused by cross-winds<sup>47</sup>.

Though the 2-input comparators inherently provide independent control of the segments of the characteristic, they are however, less attractive due to the requirement of the change in two signals at a time to affect the change in resistance and reactance axis of the characteristic.

#### 3.4.2 Multi Input Comparators :

If the pairs of input signals for the individual segments of the characteristic are so chosen that one signal amongst them is common (to be termed as operating signal) then it would be possible to compare all the pairs of

signals in one comparator, called Multi-input comparator.

Fig.3.9 illustrates a typical multi-input sine comparator, first employed by Parthasarathy<sup>32</sup>. It is evident that the phase comparison takes place between  $S_1$  and  $S_2$ ,  $S_1$  and  $S_3$  and so on. There is no 'interaction' amongst the polarising signals  $S_2, S_3$  etc. This results in independent control of individual segments of the characteristic. In this respect, this comparator has distinct advantage over the cosine comparator employed by Humpage and others<sup>19,20,22</sup> where 'interaction' took place between more than two signals resulting in loss of independent control of the segments of the characteristic.

Since, in a multi-input sine comparator, each pair of signals constituting a segment of the characteristic will have one signal in common, only  $(n+1)$  signals will be required to be compared for  $n$  segments of the characteristic.

In order to realise desired shapes of the characteristics on the impedance plane if it is found difficult to obtain the operating signal common in the pairs of signals constituting the segments of the characteristic, the unsymmetrical limits of comparison could be employed. This is described in section 3.5 .



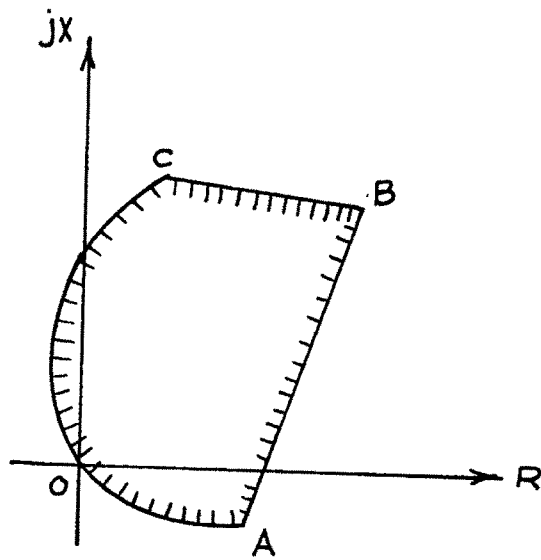


FIG. 3-10 COMPOSITE CHARACTERISTIC

Signals  $S_o$  and  $S_{p_1}$  are the operating and polarising signals respectively providing the segment ABC of the characteristic, the comparison limits being  $\beta_1$  and  $\beta_2$ .  $S_o$  and  $S_{p_2}$  are the similar signals furnishing the segment AOC of the characteristic, comparison limits being  $\beta_3$  and  $\beta_4$ .

### 3.5.2 Principle Of The Relay :

Fig.3.11 illustrates the block-schematic diagram of the first-zone relay. System quantities  $V_L$  and  $I_L$  are applied to the measuring circuit (M) which produces the required signals given by eq.(3.12). The phase shift of  $90^\circ$  in  $S_o$  is obtained by capacitor-diode combination. The pulse forming circuits  $P_1$ ,  $P_2$  and  $P_4$  produce positive going pulses from the input signals at their zero cross-overs, when they change their sign from negative to positive. Pulse from  $S_{p_1}$  is used to trigger monostable multi-vibrator circuit  $M_1$  set to provide comparison limit  $\beta_1$ . The pulse forming circuit  $P_3$  is used to derive positive going pulse from the output of  $M_1$ , at the instant when the latter starts recovering from its quasistable state. This pulse is used to trigger another multi-vibrator circuit  $M_2$  set for the comparison limit  $\beta_2$ . Thus, the output of the inverter stage (I) will be the required voltage signal to be compared with pulse from  $S_o$  to furnish segment ABC of the characteristic. Similarly another voltage signal for segment

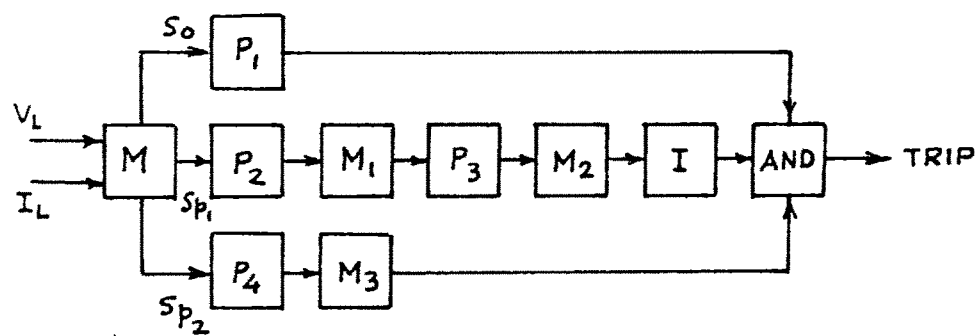


FIG. 3-11 BLOCK-SCHEMATIC DIAGRAM OF THE RELAY

AOC is obtained from the multi-vibrator circuit  $M_3$  set for the comparison limit  $\beta_3$ .

The pulse from  $S_0$  is gated by these voltage signals in the multi-input phase-comparator which is an AND gate. Multi-input phase comparator of fig.3.9 is employed for the purpose of phase comparison. Fig.3.12 shows the mode of phase comparison. It is evident that the comparator will provide the sampling pulse as an output only if at the time of its arrival in the gate both the inputs at the base of the transistor  $T_1$  are simultaneously negative [ fig.3.12 (f); (j) ; (p) and (q) ] .

The details of relay circuitry will now be explained.

### 3.5.3 Relay Circuitry :

#### Pulse Forming Circuits :

The pulse forming circuit  $P_1$  of fig.3.11 is shown in fig.3.13.  $P_2$  and  $P_4$  are similar to this circuit except that  $C_1$  is replaced by a current limiting resistor.

The required  $90^\circ$  phase shift in  $S_0$  is obtained by capacitor-diode combination  $C_1, D_1$  and  $D_2$ . The voltage shifted in phase is amplified by the transistor  $T_1$  to obtain a square wave of amplitude approximately equal to the supply voltage. The square wave is then inverted to take in to account the  $180^\circ$  phase shift due to the amplifier. The

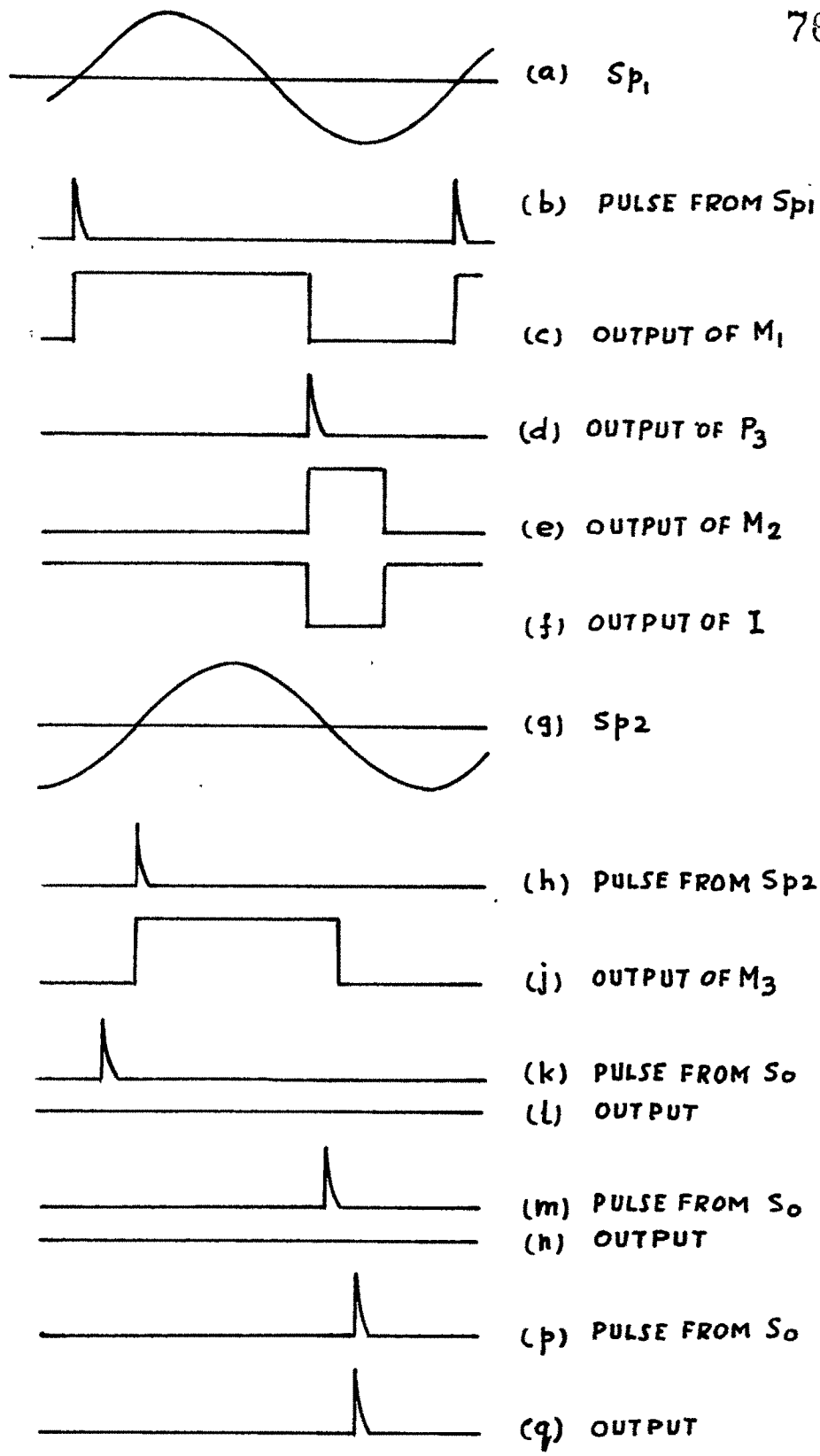


FIG. 3-12 MODE OF PHASE COMPARISON

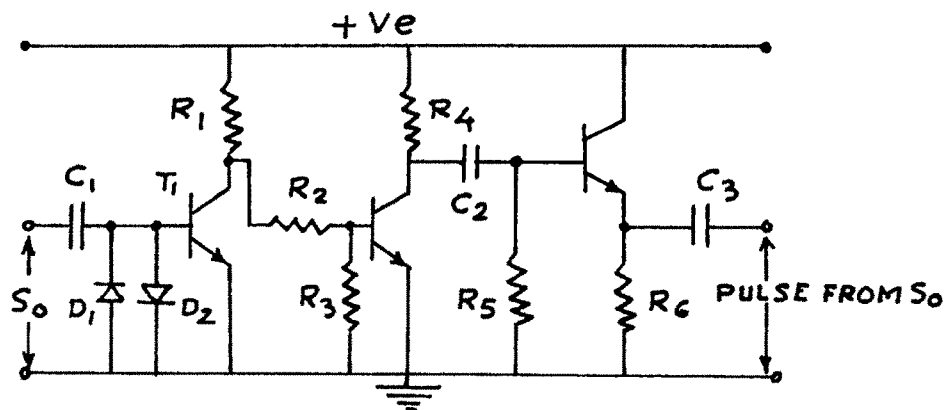


FIG. 3-13 PULSE FORMING CIRCUIT

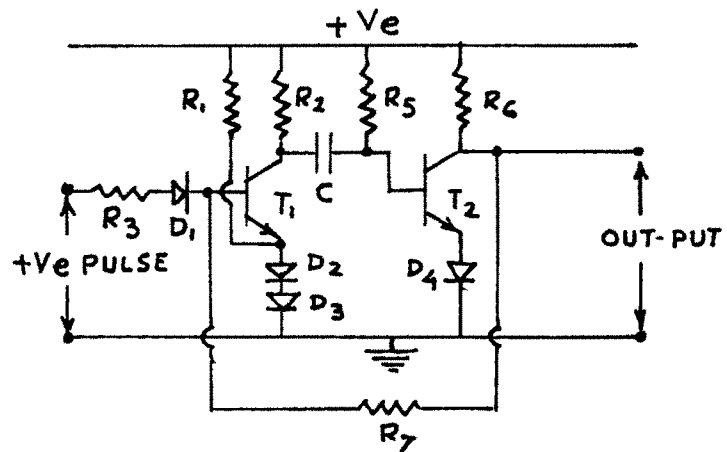


FIG. 3-14 MONOSTABLE MULTI-VIBRATOR

out-put of the inverter is differentiated employing resistance-capacitance combination ( $C_2$  and  $R_5$ ). The values of  $C_2$  and  $R_5$  are properly selected to avoid sharp pulses. The train of positive and negative pulses obtained by the differentiation of the square wave is applied to an emitter-follower circuit to eliminate the negative pulses. Capacitor  $C_3$  in the out-put stage is employed to block any d.c. voltage appearing in the train of pulses. Plates 3.1 through 3.6 illustrate the formation of positive pulses.

#### Monostable Multi-vibrator Circuits :

Fig.3.14 illustrates a typical monostable multi-vibrator circuit. Normally transistor  $T_2$  is conducting. A positive going pulse applied to the base of transistor  $T_1$  makes it conducting.  $T_2$ , therefore, stops conducting. The circuit remains in the quasi-stable state for the time given by an approximate equation

$$\tau = 0.69 R_5 C \quad \dots (3.13)$$

$\tau$  could be easily related with  $\beta$ , the angular limit of comparison. All the three multi-vibrators employed are of this type except for the specific values of  $R_5$  and  $C$ . The oscillograms of the wave forms obtained for the multi-vibrator  $M_1$  are shown in plates 3.7 and 3.8.

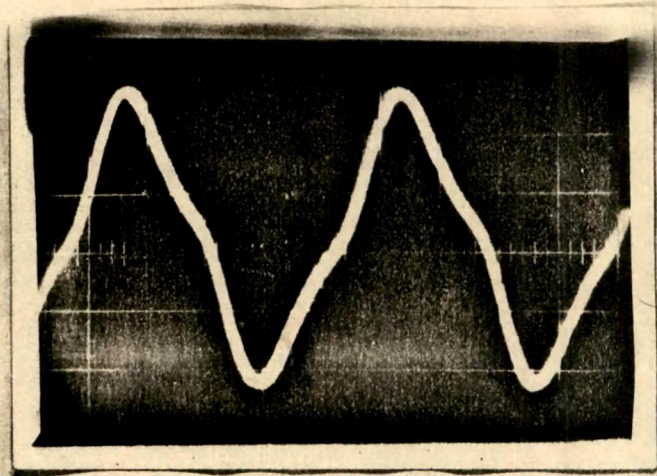


Plate 3.1  $I_{L,R}^Z$

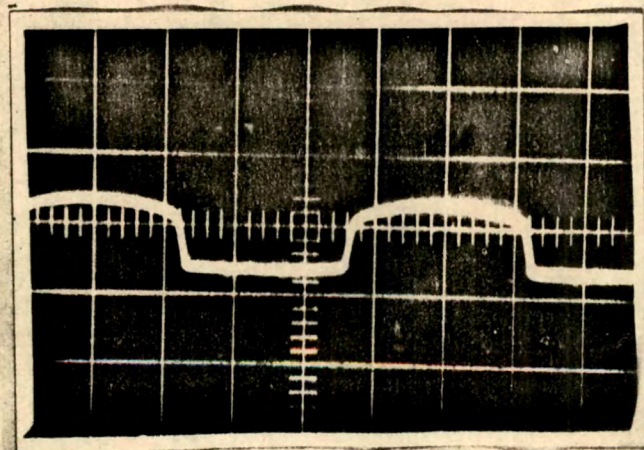
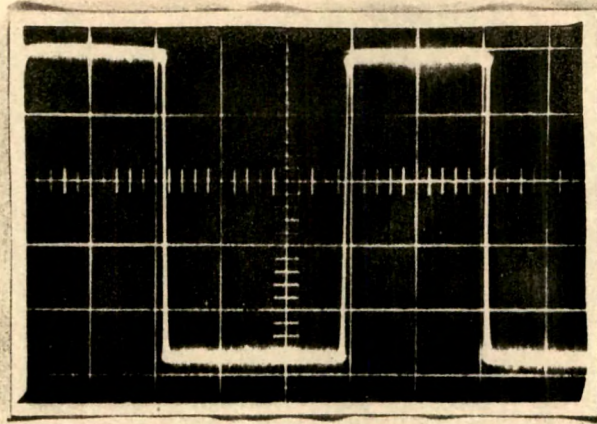
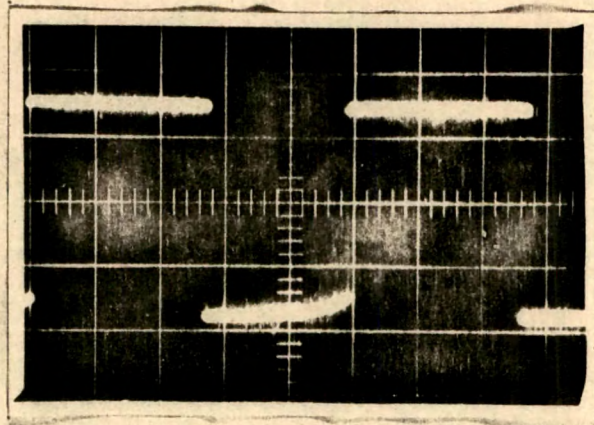


Plate 3.2 Output of Clipper



· Plate 3.3 Output of the amplifier



· Plate 3.4 Output of the inverter

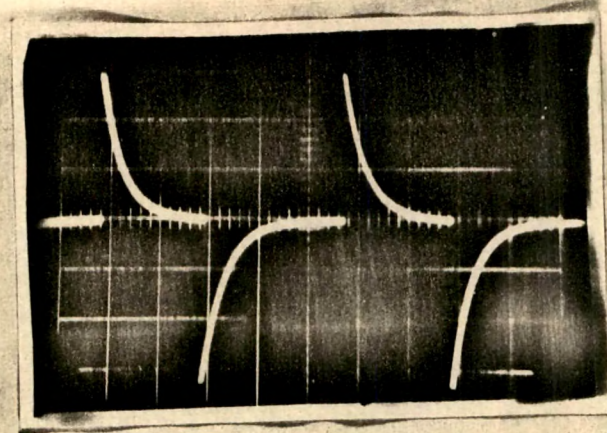


Plate 3.5 Train of positive  
and negative pulses

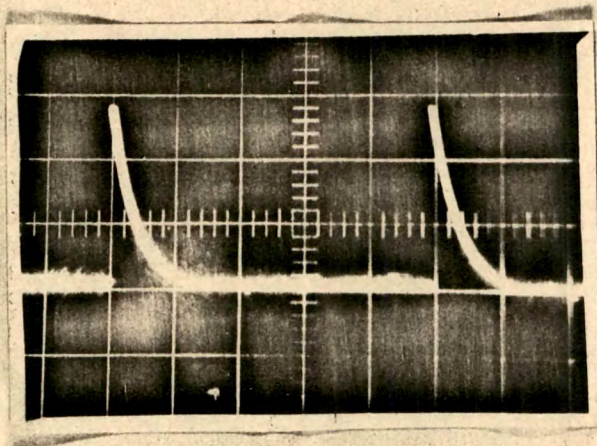


Plate 3.6 Train of positive  
pulses

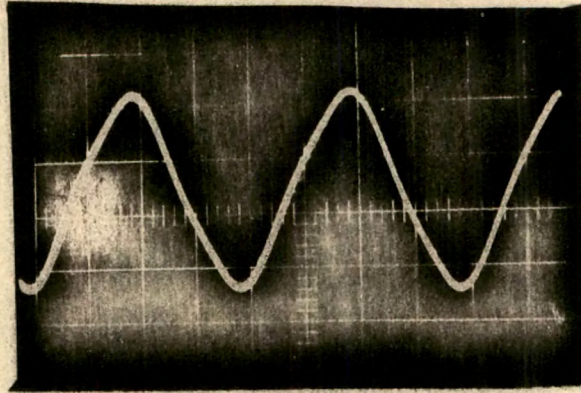


Plate 3.7 Polarising signal  $S_{p1}$

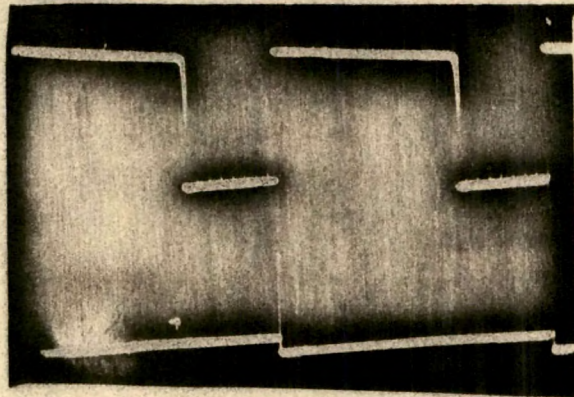


Plate 3.8 Output of Multivibrator  
with pulse input

Fig.3.15 illustrates the complete relay circuit yielding the characteristic of fig.3.10. The values of the circuit components are also marked. Plates 3.9 and 3.10 show typical printed card (front and rear view respectively). Plate 3.11 shows the complete relay model constructed during the laboratory investigation.

3.5.5 Performance Tests :

The relay described in the previous section was subjected to both steady-state and dynamic testing during the reduced scale laboratory investigation. A test-bench developed on the principle described by Hamilton and Ellis<sup>44</sup> was employed for the determination of the dynamic performance of the relay. The principle of testing and the results obtained during the tests are given in Appendix.

It is clear from the tests that the relay has very low transient over-reach (less than 6 percent) for a sufficiently large source to line impedance ratio. Further, it is evident from fig.3.12 that the phase angle measurement is done within a cycle. The relay, therefore is also fast operating.

---

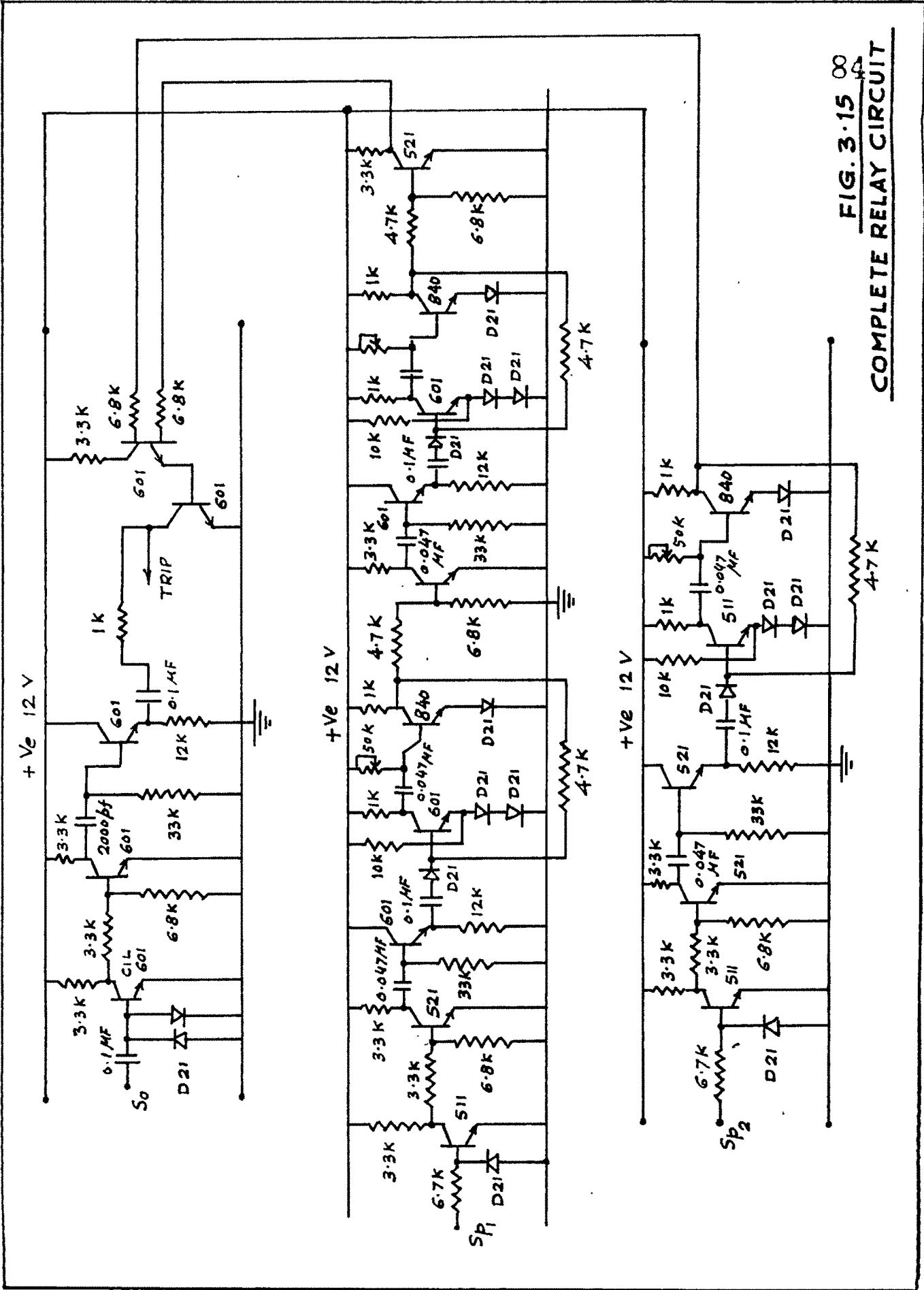
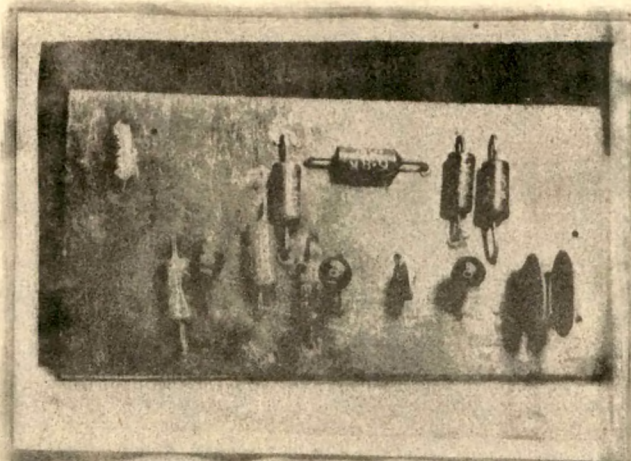
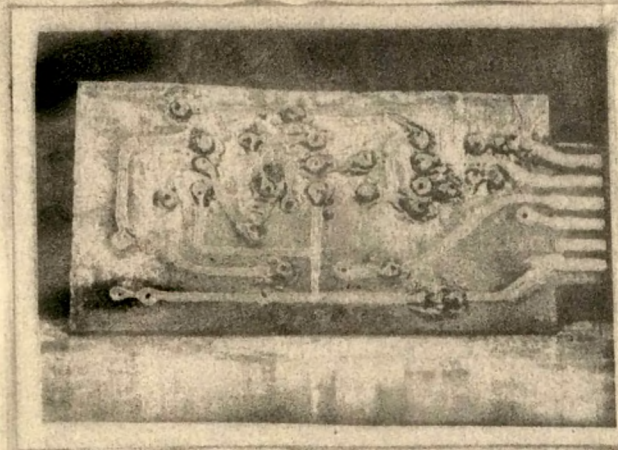


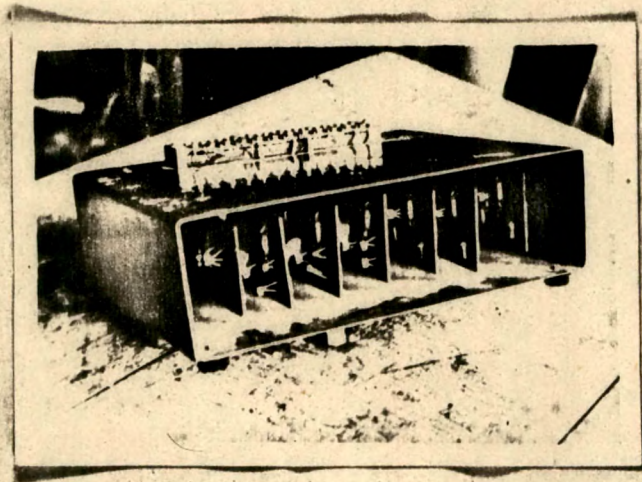
FIG. 3.15 00  
COMPLETE RELAY CIRCUIT



· Plate 3.9 Typical Printed Card  
(Front view)



· Plate 3.10 Typical Printed Card  
( Rear View )



• Plate 3.11 Complete Relay